HOMOGENEOUS NUCLEATION OF STEAM IN CONVERGENT-DIVERGENT NOZZLE

Jan Halama*, Jaroslav Fořt*

The paper is aimed at a modeling of transonic flow of steam with pressure and temperature range corresponding to conditions in steam turbines. A possibility of the droplet size spectra reconstruction is discussed. Numerical results are compared to experimental data for nozzle flow.

Keywords: *steam, nucleation, droplet size distribution, condensation, method of moments*

1. Introduction

Expansion of steam in turbines leads to non-equilibrium condensation, i.e. condensation starts when the steam temperature drops sufficiently below the saturation temperature. New droplets form either from clusters of water molecules (homogeneous nucleation) or they are created on some impurities (heterogeneous nucleation). Existing droplets grow or evaporate according to the state of surrounding vapor. Droplets appearing due to homogenous nucleation have sub-micron size and one can consider, that they are convected by the vapor. Condensation reduces thermal efficiency of turbine, changes significantly shock wave structure in the transonic flow field and can initiate pressure pulsations.

First numerical simulations of condensing steam flow appeared three decades ago, e.g. [1] or [10]. They were based on the Eulerian-Lagrangian approach. Recent works rely on the full Eulerian approach for mono-dispersed mixture, e.g. [5], [6] or [15]. Another authors, e.g. [13] or [11] use the method of moments originally published in [8], which is able to recognize the polydispersity of the mixture.

2. Flow model

Presented model is based on the work of [13]. The velocity of droplets is considered equal to the velocity of vapor. The model consists of transport equations for mass, momentum and energy of the mixture, mass fraction of liquid phase and moments for liquid phase. Mass exchange between vapor and liquid is modeled by homogeneous nucleation and droplet growth. We use three moments according to [8]

$$Q_0 = N \ , \qquad Q_1 = \sum_{i=1}^{N} r_i \ , \qquad Q_2 = \sum_{i=1}^{N} r_i^2 \ , \tag{1}$$

where N is the total number of droplets in unit mass and r_i is the radius of i-th droplet. The average droplet radius is taken as $r_{20} = \sqrt{Q_2/Q_0}$ according to [13]. The system of all

* Ing. J. Halama, Ph.D., prof. Ing. J. Fořt, CSc., Department of Technical Mathematics, Faculty of Mechanical Engineering, Czech Technical University Prague, Karlovo nám. 13, CZ-12135 Praha 2, Czech Republic

transport equations for the case of one-dimensional flow with variable cross-sectional area $A(x)$ reads

$$\frac{\partial}{\partial t}\big(A(x)\,\mathbf{W}\big) + \frac{\partial}{\partial x}\big(A(x)\,\mathbf{F}(\mathbf{W})\big) = \mathbf{P}(\mathbf{W}) + A(x)\,\mathbf{Q}(\mathbf{W}) \ , \tag{2}$$

where

$$\mathbf{W} = \begin{bmatrix} \rho \\ \rho\,u \\ e \\ \rho\,\chi \\ \rho\,Q_2 \\ \rho\,Q_1 \\ \rho\,Q_0 \end{bmatrix}, \quad \mathbf{F} = \begin{bmatrix} \rho u \\ \rho\,u^2 + p \\ (e+p)\,u \\ \rho\,\chi\,u \\ \rho\,Q_2\,u \\ \rho\,Q_1\,u \\ \rho\,Q_0\,u \end{bmatrix}, \quad \mathbf{P} = \begin{bmatrix} 0 \\ p\,A'(x) \\ 0 \\ 0 \\ 0 \\ 0 \\ 0 \end{bmatrix}, \quad \mathbf{Q} = \begin{bmatrix} 0 \\ 0 \\ 0 \\ \frac{4}{3}\,\pi\,r_\mathrm{c}^3\,J\,\rho_\mathrm{l} + 4\,\pi\,\rho\,\mathcal{M}_2\,\rho_\mathrm{l} \\ r_\mathrm{c}^2\,J + 2\,\rho\,\mathcal{M}_1 \\ r_\mathrm{c}\,J + \rho\,\mathcal{M}_0 \\ J \end{bmatrix},$$

$$\mathcal{M}_n = \int_0^\infty r^n\,N(r)\,\dot{r}(r)\,\mathrm{d}r \ .$$

The symbol ρ denotes the mixture density, u the mixture velocity, e the total energy of mixture per unit volume, p the pressure of the mixture, χ the mass fraction of liquid phase (wetness). The symbol J is used for the number of new droplets due to homogenous nucleation in unit volume per one second. The radius of these droplets is equal to the critical radius r_c. The variable ρ_l denotes the density of liquid phase. The integral $\int_{r_1}^{r_2} N(r)\,\mathrm{d}r$ equals to the number of droplets with the radius $r \in \langle r_1, r_2\rangle$ in the unit mass of mixture. The function $\dot{r}(r)$ describes the droplet growth speed. The system (2) is closed by additional equations (equation of state, material properties), for detail see [7]. The equation for pressure under the perfect gas assumption reads

$$p = \frac{(\gamma-1)\,(1-\chi)}{1+\chi\,(\gamma-1)}\left[e - \frac{1}{2}\,\rho\,u^2 + \rho\,\chi\,L\right] \ , \tag{3}$$

where the pressure p is considered the same for both vapor and liquid and L denotes the latent heat of condensation/evaporation. The specific heat ratio is taken as a function of temperature $\gamma(T) = c_\mathrm{p}(T)/(c_\mathrm{p}(T) - R_\mathrm{v})$, where R_v denotes the gas constant for vapor, $c_\mathrm{p}(T)$ the specific heat at constant pressure and T the temperature of vapor. The system (2) turns into the common single-phase flow model if $\chi = Q_0 = Q_1 = Q_2 = 0$. The original model considers the droplet growth speed calculated from average radius r_{20}, i.e.

$$\mathcal{M}_n = \int_0^\infty r^n N(r)\,\dot{r}(r_{20})\,\mathrm{d}r = \dot{r}(r_{20}) \int_0^\infty r^n N(r)\,\mathrm{d}r = \dot{r}(r_{20})\,Q_i \ . \tag{4}$$

This model is referred as AVG-P model. The modification, which is denoted as DSDF-P model, considers the log-normal distribution defined by three moments Q_0, Q_1 and Q_2 according to [9]

$$N(r) = Q_0\,\frac{1}{r\,\ln(\sigma_g)\,\sqrt{2\pi}}\,\exp\!\left(-\frac{\ln^2(r/\overline{r}_g)}{2\,\ln^2(\sigma_g)}\right) \ , \tag{5}$$

with

$$\overline{r}_\mathrm{g} = \frac{r_{20}}{\exp(0.5\,\ln^2(\sigma_g))} \ , \quad \sigma_\mathrm{g} = \exp\sqrt{\ln(c_\mathrm{v}^2+1)} \ , \quad r_{20} = \sqrt{\frac{Q_2}{Q_0}} \ , \quad c_\mathrm{v} = \sqrt{\frac{Q_0\,Q_2}{Q_1^2} - 1} \ . \tag{6}$$

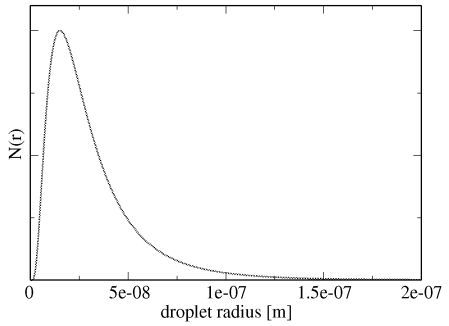

Fig.1: Example of log-normal droplet size distribution

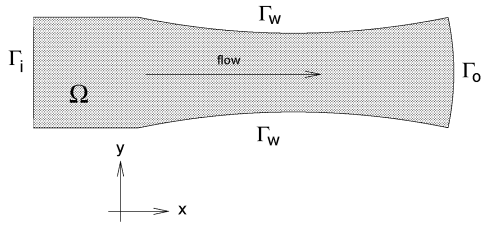

Fig.2: Solution domain – nozzle

3. Numerical solution

Consider a convergent-divergent nozzle, see the Fig. 1, with subsonic flow at the inlet boundary Γ_i. Six parameters are set at Γ_i according to the 1D theory of characteristics of linearized problem (total temperature T_0, total pressure p_0, wetness χ and moments Q_0, Q_1 and Q_2). The flow is supersonic at the outlet boundary Γ_o, therefore according to the 1D theory of characteristics for linearized problem one cannot prescribe any condition at Γ_o.

The numerical method has to cover very different time scales of convection, nucleation and droplet growth. Numerical method is therefore based on the splitting method of [14]. The splitting method allows the use of different time discretization for individual phenomena. The splitting method has three successive steps

$$\frac{\partial}{\partial t}\mathbf{W}^* = \mathbf{Q}(\mathbf{W}^*) \;, \tag{7}$$

$$\frac{\partial}{\partial t}\big(A(x)\,\mathbf{W}^{**}\big) = -\frac{\partial}{\partial x}\big(A(x)\,\mathbf{F}(\mathbf{W}^{**})\big) + \mathbf{P}(\mathbf{W}^{**}) \;, \tag{8}$$

$$\frac{\partial}{\partial t}\mathbf{W}^{***} = \mathbf{Q}(\mathbf{W}^{***}) \;, \tag{9}$$

where the Eq. (7) is solved with initial data $\mathbf{W}^*(t) = \mathbf{W}(t)$, the Eq. (8) with initial data $\mathbf{W}^{**}(t) = \mathbf{W}^*(t + \Delta t/2)$ and the Eq. (9) with initial data $\mathbf{W}^{***}(t) = \mathbf{W}^{**}(t + \Delta t)$. The value $\mathbf{W}^{***}(t + \Delta t/2)$ approximates the solution $\mathbf{W}(t + \Delta t)$ of the original system (2). The single step of the Lax-Wendroff finite volume method is applied for the solution of (8) and several steps of the Runge-Kutta method is used to solve (7) and (9).

4. Numerical results

Consider the Barschdorff nozzle [2], see the Fig. 2, discretized by 200 cells with the spacing $1.4{\times}10^{-3}$ in the convergent-divergent part. The inlet total pressure is 78390 Pa,

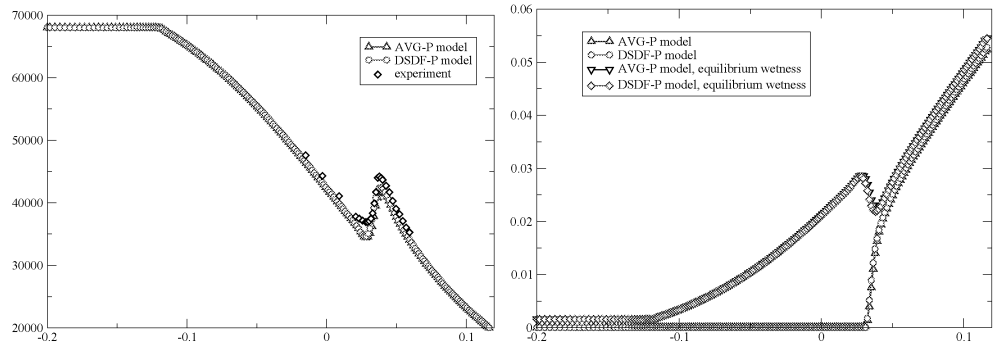

(a) pressure (b) wetness

Fig.3: Pressure and wetness along nozzle axis, experimental data from [2]

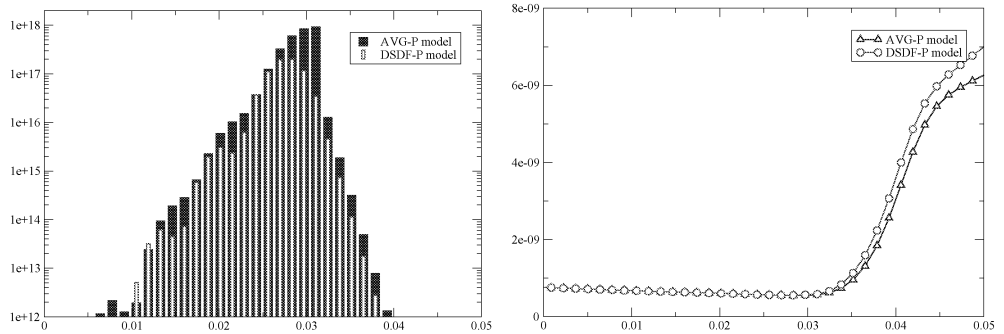

(a) $Q_0(x_i) - Q_0(x_{i-1})$ (b) critical radius

Fig.4: Increments of number of droplets $Q_0(x_i) - Q_0(x_{i-1})$ and critical radius r_c within the nucleation zone in grid points x_i

the inlet total temperature is 373.1 K and the steam does not contain the liquid phase at the inlet (i.e. $Q_0 = Q_1 = Q_2 = \chi = 0$). The Figure 3 shows the graphs of pressure and wetness along the nozzle axis for both AVG-P flow model (droplet growth computed using the average radius r_{20}) and DSDF-P flow model (droplet growth computed using log-normal distribution of droplet size). The Figure 4(a) shows how many droplets appears due to homogenous nucleation in each grid point and the Figure 4(b) shows the size (critical radius) of these new droplets. Nucleation takes place in a relatively small region and it almost cancels the thermodynamic non-equilibrium, see the difference between wetness and the equilibrium wetness in the Figure 3(b). Nucleation stops around $x = 0.04$ and the condensation follows more-less the equilibrium case from that point. The nucleation releases a non-negligible amount of the latent heat in a relatively small region, it yields the so called nucleation shock, see the pressure rise around $x = 0.03$ in the Figure 3(a). Both models yield nearly the same results for pressure and wetness distributions. However they differ significantly in the composition of the droplet spectra. The DSDF-P model gives smaller total amount of droplets Q_0 at the nozzle outlet, see the Table 1. The DSDF-P model yields slightly higher wetness, so the DSDF-P model predicts 'bigger droplets'. The average radius r_{20} is not a good parameter to compare DSDF-P and AVG-P models from the point of the average droplet size, see comparison of different droplet size averages in the Table 2, where r_{10} is the linear average radius, r_{20} is the surface average radius, r_{30} is the volume average radius and the r_{32} is the Sauter mean radius.

	Q_0	Q_1	Q_2	χ
AVG-P model	9.45×10^{17}	2.16×10^{10}	515.28	0.0523
DSDF-P model	7.12×10^{17}	0.72×10^{10}	225.16	0.0527

Tab.1: Parameters of liquid phase at the nozzle outlet

	$r_{10}=Q_1/Q_0$	$r_{20}=\sqrt{Q_2/Q_0}$	$r_{30}=\sqrt[3]{Q_3/Q_0}$	$r_{32}=r_{30}^3/r_{20}^2$
AVG-P model	$2.28\cdot10^{-8}$	$2.33\cdot10^{-8}$	$2.36\cdot10^{-8}$	$2.42\cdot10^{-8}$
DSDF-P model	$1.01\cdot10^{-8}$	$1.77\cdot10^{-8}$	$2.61\cdot10^{-8}$	$5.67\cdot10^{-8}$

Tab.2: Different average radii of droplets at the nozzle outlet

5. Conclusions

Presented results show, that the model DSDF-P could be a good option for more detailed modeling of droplet size spectra. The results also show, that one has to be very careful when computing the average size of droplet. The original model AVG-P has the average size of droplets nearly independent of definition, it means that AVG-P model yields nearly monodispersed mixture. The average size of droplet for the DSDF-P model strongly depends on the used definition.

Acknowledgment

The support of grant GA ČR 101/11/1593 is gratefully acknowledged.

References

[1] Bakhtar F., Tochai Mohammadi M.T.: An investigation of two-dimensional flow of nucleating and wet steam by the time-marching method, Int. J. Heat Fluid Flow 2, 5–18, 1980

[2] Barschdorff D.: Verlauf der Zustandgroessen und gasdynamische Zusammenhaenge der spontanen Kondensation reinen Wasserdampfes in Lavaldüsen, Forsch. Ing.-Wes. 37(5), 1971

[3] Becker R., Döring W.: Kinetische Behandlung der Keimbildung in übersättingten Dämpfen, Ann. d. Physik 24(8), 1935

[4] Dobeš J., Fořt J., Fürst J., Halama J., Kozel K.: Numerical modeling of unsteady flow in steam turbine cascade. Journal of Computational and Applied Mathematics 234(7), 2336–2341, 2008

[5] Dykas S., Goodheart K., Schnerr G.H.: Numerical study of accurate and efficient modelling for simulation of condensing flow in transonic steam turbines, 5th European conference on Turbomachinery 751–760, 2003

[6] Gerber A.G., Kermani M.J.: A pressure based eulerian–eulerian multi-phase model for non-equilibrium condensation in transonic steam flow, International Journal of Heat and Mass Transfer 47, 2217–2231, 2004

[7] Halama J., Benkhaldoun F., Fořt J.: Flux schemes based finite volume method for internal transonic flow with condensation, International Journal for Numerical Methods in Fluids 65(8), 953–968, 2011

[8] Hill P.G.: Condensation of water vapor during supersonic expansion in nozzles, Journal of Fluid Mechanics 3, 593–620, 1966

[9] John V., Angelov I., Önc'ül A., Thevenin D.: Techniques for the reconstruction of a distribution from a finite number of its moments, Journal Chemical Engineering Science 62(11), 2890–2904, 2007

[10] Moheban M., Young J.B.: A time-marching method for the calculation of blade-to-blade non-equilibrium wet steam flows in turbine cascades, IMechE conference on computational methods in turbomachinery paper C76/84, 89–99, 1984

[11] Mousavi A., Gerber A.G., Kermani M.J.: Representing polydispersed droplet behavior in nucleating steam flow with the quadrature - method - of - moments, 2006 ASME Joint U.S.-European Fluids Engineering Summer Meeting
[12] Petr V., Kolovratník M.: Heterogeneous effects in the droplet nucleation process in LP steam turbines, 4th European Conference on Turbomachinery
[13] Šejna M., Lain J.: Numerical modelling of wet steam flow with homogenous condensation on unstructured triangular meshes, Journal ZAMM 74(5), 375–378, 1994
[14] Strang G.: On the construction and comparison of difference schemes, SIAM Journal of Numerical Analysis 5, 506–517, 1968
[15] Sun L., Zheng Q., Liu S.: 2d-simulation of wet steam flow in a steam turbine with spontaneous condensation, Journal of Marine Science and Application 6(2), 59–63, 2007

Received in editor's office: July 26, 2013
Approved for publishing: December 1, 2013